

Utah State University

DigitalCommons@USU

Undergraduate Honors Capstone Projects

Honors Program

5-2009

Polar Mesospheric Clouds: A Satellite and Ground-Based Comparison

Jodie Barker-Tvedtnes
Utah State University

Follow this and additional works at: <https://digitalcommons.usu.edu/honors>



Part of the [Physics Commons](#)

Recommended Citation

Barker-Tvedtnes, Jodie, "Polar Mesospheric Clouds: A Satellite and Ground-Based Comparison" (2009).
Undergraduate Honors Capstone Projects. 21.
<https://digitalcommons.usu.edu/honors/21>

This Thesis is brought to you for free and open access by the Honors Program at DigitalCommons@USU. It has been accepted for inclusion in Undergraduate Honors Capstone Projects by an authorized administrator of DigitalCommons@USU. For more information, please contact digitalcommons@usu.edu.



**POLAR MESOSPHERIC CLOUDS:
A SATELLITE AND GROUND-BASED COMPARISON**

by

Jodie Barker-Tvedtnes

**Thesis submitted in partial fulfillment
of the requirements for the degree**

of

DEPARTMENTAL HONORS

in

**Physics with a Professional Emphasis
in the Department of Physics**

Approved:

Thesis/Project Advisor
Dr. Michael J. Taylor

Departmental Honors Advisor
Dr. David Peak

Director of Honors Program
Dr. Christie Fox

**UTAH STATE UNIVERSITY
Logan, UT**

Spring 2009

Abstract

Polar Mesospheric Clouds (PMCs) are tenuous ice clouds that form near the cold ($<150\text{K}$) summer mesopause region (80-85 km). From the ground, these clouds are seen during twilight hours as Noctilucent or “night shining” Clouds (NLCs) and are typically seen from latitudes from 50° to 65° . Observations by the Solar Backscatter Ultraviolet (SBUV) instruments on the NOAA satellites have shown that the occurrence and brightness of NLCs have been increasing over the last three decades prompting speculation concerning their possible role in climate change. Recently the Aeronomy of Ice in the Mesosphere (AIM) satellite was launched (April 2007) and is the first satellite dedicated to the study of NLCs. In this report, we compare SBUV and AIM PMC observations with ground-based image data collected during two campaigns from Edmonton, Canada (June 30-July 17, 2007) and Delta Junction, Alaska (July 29-August 17, 2007). Four nights of data are discussed where coincident measurements were obtained by AIM, SBUV/2 and ground-based imagers. The results show good spatial or temporal agreement, but rarely both, and illustrate the importance of coordinated measurements for better understanding the geographic and local time variability of PMCs. Initial studies using data from the Ozone Monitoring Instrument (OMI) on the AURA satellite are also presented.

Acknowledgements

I would like to first acknowledge and to thank my advisor Dr. Michael Taylor for the opportunity to conduct this research and for all of his help and guidance throughout this project. I would also like to thank Dr. Matthew DeLand for providing the SBUV/2 and OMI satellite data, and Dr. David Rusch and the CIPS Science Team for the AIM CIPS data, which made this research possible.

This research has been funded, in part, by the NASA AIM Satellite Mission, a Willard L. Eccles Undergraduate Research Fellowship (2007-2008), and a College of Science Summer Mini-Grant (2006). Additional funding came from the Society of Physics Student (SPS) for presentations of this research at the 2008 AGU Fall Meeting in San Francisco, CA and the 2008 International Conference for Physics Students in Krakow, Poland.

Above all I would like to thank my daughter, Kalila, for all of her patience and support throughout this research and my undergraduate career.

Table of Contents

1. Background	7
2. Ground-Based Measurements of PMC/NLC	9
2.1. Imaging	9
2.2. Rockets	10
2.3. Lidar	11
2.4. Radar	11
3. Satellite Measurements of PMC	12
3.1. Solar Backscatter Ultraviolet (SBUV/2) Instruments	13
3.2. Ozone Monitoring Instrument (OMI)	14
3.3. Aeronomy of Ice in the Mesosphere (AIM)	15
4. Ground-Based NLC Campaigns	16
4.1. Canada (June 31-July 14, 2007)	16
4.2. Alaska (June 23-August 18, 2007)	17
5. Analysis and Results	18
5.1. Ground-Based Data Analysis	18
5.2. Satellite Comparisons	19
5.2.1. Comparison of OMI and SBUV/2	19
5.2.2. AIM and SBUV/2	20
5.3. Satellite and Ground-Based Data	22
5.3.1. Canadian Comparison	23
5.3.2. Alaskan Comparison	25
6. Summary	26
7. Conclusions	27
8. Future Research	28
8.1. Investigation of the 5-day wave in OMI data	28
8.2. NEW OMI / AIM Global Study	28
8.3. Investigation of the Gap	29
8.4. New Low Latitude OMI Investigation	29
8.4.1. Logan, UT, July 4/5, 2008 (day 186)	29
9. References	30
10. Author's Biography	32

Table of Figures

Figure 1 An image of a noctilucent cloud from Donnelly Dome, just south of Fairbanks Alaska. Photograph by Dan Burton USU August 10/11 2007.....	7
Figure 2 PMC albedo in units of $1 \times 10^{-6} \text{ str}^{-1}$ and frequency of occurrence are plotted versus days from solstice at a single longitude band (180°). (Merkel et al. 2009).....	7
Figure 3 An atmospheric profile from the troposphere through the lower thermosphere. The red line shows the temperature variation with height. Courtesy Dr. Jon Schrage, Purdue University.	8
Figure 4 Composite image showing NLC observed from Logan, UT (41.7°N) on the night of 22/23 June 1999 at 04:30 UT. (Taylor et al., 2002)	8
Figure 5 Geometry for viewing NLC from the Ground. Θ is the solar depression angle ($\sim 6^\circ$ to 16° below the horizon).	9
Figure 6 Classifications of NLCs (Gadsden and Parviainen, IAGA Report, 1995)	10
Figure 7 Lidar data showing an NLC profile from the Rayleigh lidar located at the Poker Flat Research Range just north of Fairbanks, AK. Courtesy Richard Collins, University of Alaska, Fairbanks.	11
Figure 8 An example of Radar data from PFISR, incoherent scatter radar located at the Poker Flat Research Range. Courtesy Craig Heinselman, SRI	11
Figure 9 A typical background-corrected picture of polar mesospheric clouds observed by a ultraviolet imager on the MSX Satellite. (Carbary et al. 2003)	12
Figure 10 NLC photographed by the Expedition 17 crew on the International Space Station on July 22, 2008 when the station was located ~ 340 km over western Mongolia. Courtesy NASA.	12
Figure 11 Summary PMC data collected from the SBUV/2 instrument on the NOAA 18 satellite. The boxes indicate the spatial extent of each scan and the fill color indicates the residual albedo of a PMC detection.	13
Figure 12 Comparison of the albedo (left) and albedo residual (right) derived from the SBUV/2 cloud detection algorithm as a function of solar zenith angle for the NOAA-17 SBUV/2 data from 20 July 2007. Albedo and albedo residual units on all plots are 10^{-6} sr^{-1} . Black, closed circles denote non-cloud points; gray, plus symbols represent cloud detections. (the latitude range is indicated in the left panel.) The white line in the left panels indicates a fourth order polynomial fit to the background enabling the residuals to be determined. (Benze et al. 2008).	13
Figure 13 An example of PMC data collected by the Ozone Monitoring Instrument for a 24 hour period on July 10, 2005.	14
Figure 14 A 24 hour summary “daisy” plot from the CIPS instrument. July 5, 2007... ..	15
Figure 15 An individual scene from the CIPS UV imager on the AIM satellite. Color variations indicate the intensity of the light scattered by the clouds.	15

Table 1 A summary of the nights for which data were collected during the Campaign in Canada during the summer of 2007.....	16
Figure 16 A Stereo Image Pair taken on July 5 2007 at 05:49:28 UT from Namao and Beaver Creek in Alberta, Canada.....	17
Figure 17 The site geometry for the NLC campaign in Alaska. (Courtesy Google) Images were being taken of the same cloud structures which were recorded by the lidar and radar at PFRR.....	17
Figure 18 An example of the NLC data collected during the campaign in Alaska. The images are from the night of August 10/11 and the parallax between the two sites is indicated by the arrows. The circles indicate the common star field in each image.....	18
Figure 19 (Left) Two-station images of an NLC un-warped and projected onto a geographic map. The images were taken on August 10/11 at 2:00 LT from Donnelly Dome and the Girstle River. (Right) The original image of the NLC taken from the site on the Girstle River.....	18
Figure 20 Comparison of SBUV and OMI data for a 24 hour period (day 200). The open boxes indicate SBUV/2 PMC detections while the diamonds indicate OMI PMC detections.	19
Figure 21 Comparison ‘daisy’ plots for day 190, 200, and 223. The SBUV data are seen as open boxes over the AIM ‘daisy’ for each 24-hour period.	20
Figure 22 Example data from the comparison using individual AIM orbits and the corresponding SBUV measurements. The images on the right are enlargements of the data in the yellow boxes in the images on the left. Each of these orbits shows excellent agreement between the SBUV PMC detections and the AIM PMC data.....	22
Table 2 The results for the AIM / SBUV/2 comparison for days 190, 200, and 223 during the 2007 NLC season.	22
Figure 23 Data collected on the night of July 1/2 2007. Right: The SBUV data, shown by the red and pink dots, extends directly over the imaging sites ~2 hrs after imaging ceased. Left: NLC image taken at 9:46 UT from Namao by Mark Zalcik (CanAM Coordinator).....	23
Figure 24 OMI data for day 183. The box indicates the location of Edmonton Canada, the light lines indicate faint PMC detections and the dark lines indicate strong PMC detections over a range of 10° in both latitude and longitude.	24
Figure 25 OMI Data for day 185. The box indicates the location of Edmonton Canada, the light lines are faint PMC detections and the dark lines indicate strong PMC detections.	24
Figure 26 Data collected for the night of the 4/5 of July. Left: The unwarped ground-based image mapped with temporally coincident SBUV/2 detections. Right: NLC image taken at 5:49 UT from Namao, Canada by Mark Zalcik.	24
Figure 27 Spatially coincident OMI / ground-based data for August 10/11, 2007. The box indicates the location of PFRR, dark lines are PMC detections, light lines are faint detections.	25

Figure 28 Two station images mapped with the coincident SBUV/2 detections for the night of August 10/11.	25
Figure 29 A data comparison for the night of the 10/11 of August 2007. The color bar indicates the intensity of the AIM PMC signal while the pink and red dots indicate SBUV detections from both the NOAA 16 and 18 Satellites. The ground-based NLC data has been un-warped to show the geographic location of the NLC display.	26
Figure 30 Examples of longitudinal variation and 70° N and 75° N in OMI PMC data for the nights of July 20 and 21 2007.	28
Figure 31 OMI data from orbit 21109 on day 185 show spatial coincidence with visual and imaging reports from Logan UT (41°N, 111°W) and Rexburg ID (43.5°N, 111.5°W). The photograph below was taken from Rexburg, ID by B. R. Jordan.	29

1. Background

Polar mesospheric clouds (PMCs) are a beautiful and mysterious high-latitude summertime phenomenon that was first observed in 1885. They are the highest clouds on earth occurring at ~ 82 km, at the very edge of space (Gadsden and Schroder, 1989). From the ground, these clouds are seen during twilight hours as Noctilucent or “night shining” Clouds (NLCs) and are typically seen from latitudes from 50° to 65° . Due to their great height these clouds have provided valuable data on the dynamics of the upper atmosphere. Most importantly, in recent decades, satellite data have shown that their occurrence frequency and brightness have increased measurably (Deland et al., 2007), raising speculation concerning their role as indicators of significant changes in climate in the upper atmosphere (Thomas, 1996).



Figure 1 An image of a noctilucent cloud from Donnelly Dome, just south of Fairbanks Alaska. Photograph by Dan Burton USU August 10/11 2007.

The first reported observations of Noctilucent Clouds (NLC) were made over 100 years ago independently by Robert Leslie and T.W. Backhouse during the summer of 1885, two years after the devastating eruption of Krakatoa, an island in Indonesia. In his letter to the editor in *Nature* Leslie (1885) describes these clouds with the following statement:

“These clouds were wave-like in form, and evidently at a great elevation, and though they must have received their light from the sun, it was not easy to think so, as upon the dark sky they looked brighter and paler than clouds under a full moon.” (Leslie, 1885)

The first photograph and height measurements were made using triangulation techniques two years later from Germany by Otto Jesse (1887). The season for viewing NLC begins in mid-May and goes through to mid-August in the northern hemisphere. In the southern hemisphere the season is ~ 2 weeks shorter extending from mid-November to mid-February. Since the first sightings there have been numerous reports of NLC seasonally

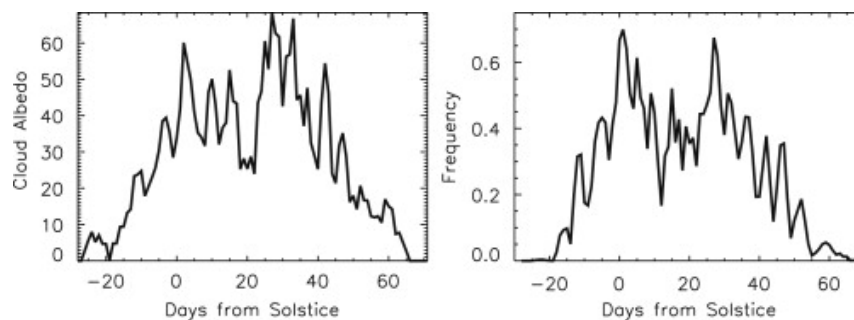


Figure 2 PMC albedo in units of $1 \times 10^{-6} \text{ str}^{-1}$ and frequency of occurrence are plotted versus days from solstice at a single longitude band (180°). (Merkel et al. 2009)

from Europe, Russia, and/or Canada. A typical NLC season is shown in Figure 2 with the cloud albedo and frequency plotted versus days from solstice. It remains a mystery why these clouds weren't reported earlier. One hypothesis is that increasing methane associated with the industrial revolution helped push the clouds into the visible realm. (Thomas, 1996).

The motivation for studying NLC/PMC arises from the fact that over the past few decades there have been notable changes in their brightness, occurrence frequency and lower latitudinal extent. Taylor et al. (2002) and Zalcik (1998) have shown that, although these clouds were initially a polar phenomena, over the past few decades there has been a tendency for them to be seen at significantly lower latitudes. In addition to the clouds moving equatorward, Deland et al. (2003, 2007) shows that satellite data indicate that PMC occurrence frequency and brightness have increased measurably over the past 30 years. These changes have lead to speculation concerning their role as indicators of significant changes in climate in the upper atmosphere (Thomas, 1996). The reason for this connection is the sharp drop in the atmospheric temperature in the summer mesopause along with an inverse relationship between the temperature of the lower and upper atmosphere. The summertime temperature profile seen in Figure 3 reveals a strong minimum in the Mesopause (~85 km). During the PMC season the temperatures in this region reach a minimum of <140K (-133°C). Surprisingly, as the troposphere and stratosphere heat up during the summer months the mesopause reaches lower and lower temperatures making it the coldest place on earth.

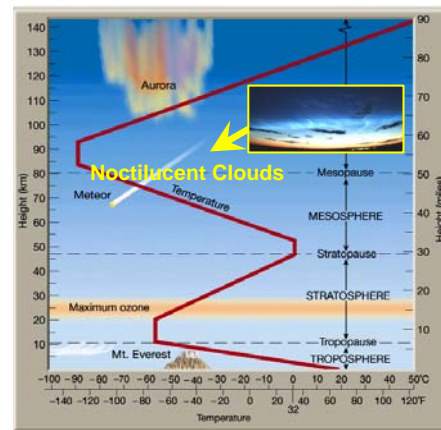


Figure 3 An atmospheric profile from the troposphere through the lower thermosphere. The red line shows the temperature variation with height. Courtesy Dr. Jon Schrage, Purdue University.

In 1995 there was an NLC occurrence at 41°N in Logan UT which was documented by

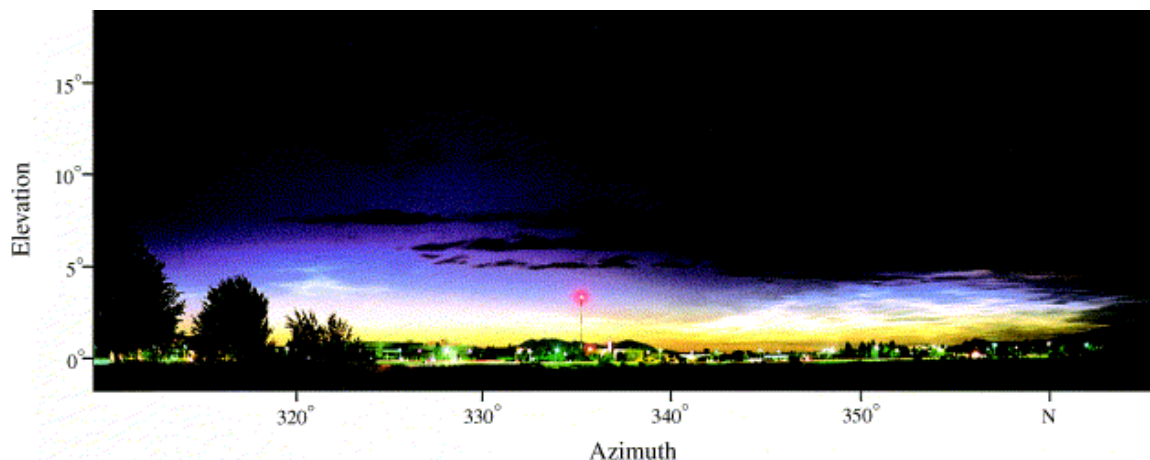


Figure 4 Composite image showing NLC observed from Logan, UT (41.7°N) on the night of 22/23 June 1999 at 04:30 UT. (Taylor et al., 2002)

lidar and again in 1999 which was documented by both lidar and imaging equipment. A photograph of this display can be seen in Figure 4. This is a major indication of a continuing trend in NLC formation which has caused concern among many scientists. The NLC boundaries appear to have been moving equatorward over the past few decades. This may be explained by an increase in the CO₂ concentration in the lower atmosphere which acts to lower the temperature in the mesopause region. Furthermore, the amount of water vapor in the upper atmosphere may have increased over the past century due to increased amounts of methane being released into the lower atmosphere, due to farming, which is then converted to water vapor through chemical reactions as it is transported upward through the stratosphere into the mesosphere. A temperature decrease of ~7 K over the past 100 years in the mesopause region would be needed to account for the observed NLC change. (Gadsden and Taylor, 1994). Furthermore, modeling studies have shown that if the CO₂ content in the lower atmosphere doubled, based on its conditions in 2003, the NLC boundary would be lowered to ~35° which would make the clouds visible to a majority of the human population (Deland et al., 2003).

2. Ground-Based Measurements of PMC/NLC

2.1. Imaging

From the ground NLC can be viewed within the twilight arch when the sun is typically between 6° and 16° below the horizon. This puts the observer in darkness while the clouds are still illuminated by sunlight. The geometry for this can be seen in Figure 5. This particular geometry is demanded by the fact that NLC are so tenuous. The light scattered from the clouds cannot compete with Rayleigh scattered sunlight during the daytime.

When viewing NLC there are some distinct structures which can be observed. The main structures are divided into 4 categories which are Type I: veils, Type II: bands, Type III: billows and Type IV: whirls. Examples of these categories can be seen in Figure 6. Typically displays have a variety of these structures as well as other structures which do not fit into the defined categories, such as rings. The AIM satellite (discussed in the next section) has revealed large ring-like structures at high latitudes. The bands which are large-scale structures have been shown to have wavelengths of ~10-100 km and are thought to be due to temperature variations in the mesopause region caused by propagating atmospheric gravity waves. Billows are smaller scale structures with wavelengths of ~3-10 km. These waves are mainly attributed to strong wind shears causing short lived dynamic instabilities (Kelvin-Helmholtz waves). Jensen and Thomas (1998)

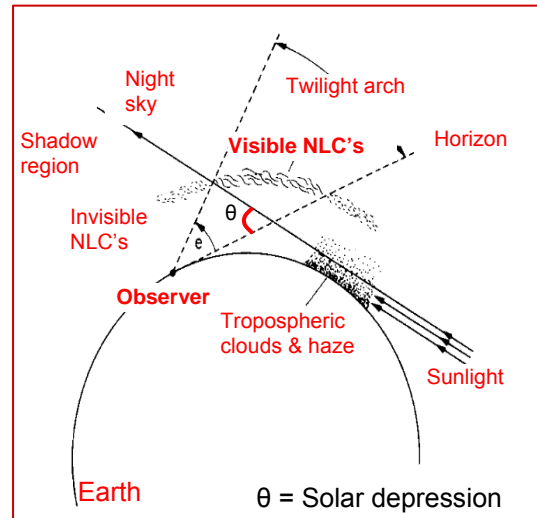


Figure 5 Geometry for viewing NLC from the Ground. θ is the solar depression angle (~6° to 16° below the horizon).

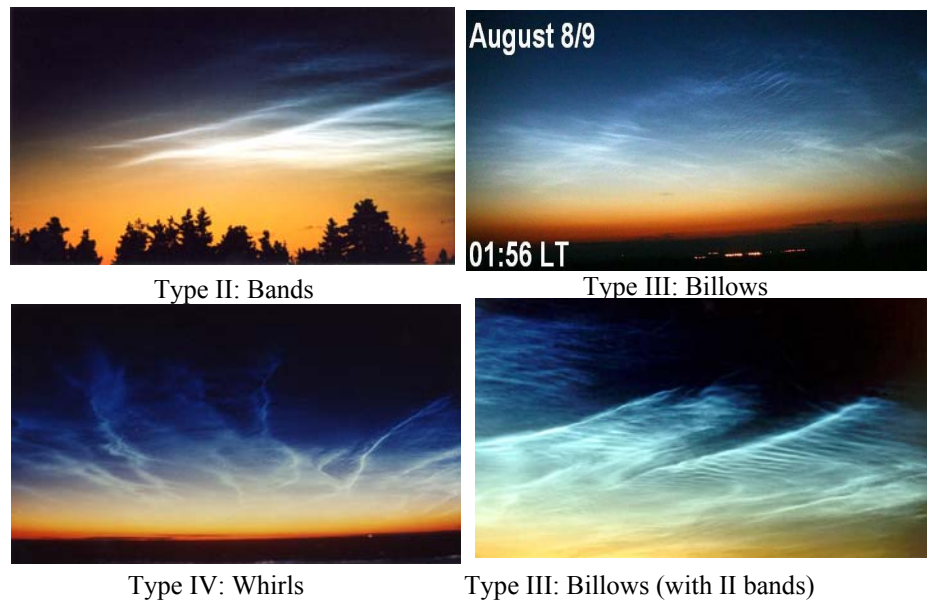


Figure 6 Classifications of NLCs (Gadsden and Parviainen, IAGA Report, 1995)

determined that the mean mesopause temperature must be about 5 K colder for NLC to form when atmospheric waves are present. The same study also determined that long-period (>10 hours) waves may enhance the brightness of existing NLC temporarily but they will not induce the formation of the clouds. In 2002, evidence was found which indicated that there is also a correlation between the effects of 5-day planetary waves and ground-based observations of NLC (Kirkwood and Stebel, 2002).

There have been several methods used to study NLC/PMC over the past centuries. Initially ground-based imaging and triangulation was used to gather data on the height and the size of various structures as mentioned above. These methods have been improved upon and carried into current studies. Other methods include rocket soundings, lidar, radar, and, satellite measurements. Initially it was not clear that the phenomena seen by these individual instruments were the same but comparative studies in the past decade have shown that we are in fact looking at different pieces of the same overlying phenomena.

2.2. Rockets

The first rocket was launched in on August 7, 1962 from Kronogard, Sweden. (Hemenway et al., 1964) In general rocket measurements are the only way to get in situ measurements on NLC since planes cannot fly high enough and satellites orbit at much greater altitudes than those at which NLC occur. In the 1960's a series of rocket measurements were used to determine that the NLC particles may have been ice coated dust particles. (Hemenway et al. 1964)

Rockets have also been used to measure atmospheric temperature profiles as well as the height of NLC. The main problem with this type of investigation of NLC is that rockets only sample a small region for a very brief amount of time. Rocket measurements have, nevertheless, yielded some very important results concerning the NLC particles themselves.

2.3. Lidar

Lidar techniques have been widely used to study several different aspects of NLC. These include determination of the particle sizes, the thickness of the NLC layer, the presence of waves in the clouds, temperature profiles, brightness variations using the intensity of the scattered signal, and of course, height measurements. At latitudes greater than 65° , where the PMC are more frequent, lidar is especially important since the sun never drops low enough below the horizon for the clouds to become visible. As the lidar does not depend on the sun to view the clouds it is possible to gather data on NLC throughout the summer months (provided the skies are clear). Some lidar systems, such as the one located at the Arctic Lidar Observatory (ALOMAR), in northern Norway, have been collecting data on NLC for a couple of decades leading to long lived coherent data sets which can offer a great deal of information on trends in the observed NLC properties.

An example of lidar data for the night of August 10/11 2007 can be seen in Figure 7. On this night NLC were clearly detected by both Rayleigh (and Iron) lidar systems located at the Poker Flat Research Range just north of Fairbanks Alaska from 01:00 to 04:00 LT. The NLC showed height variations of 83 to 85 km during the night and the peak Rayleigh backscatter coefficient was $\sim 15 \times 10^{-10}$ (m⁻¹/sr) indicating a strong NLC display. A strong (sporadic) iron layer was also detected between 93 and 98 km (not shown).

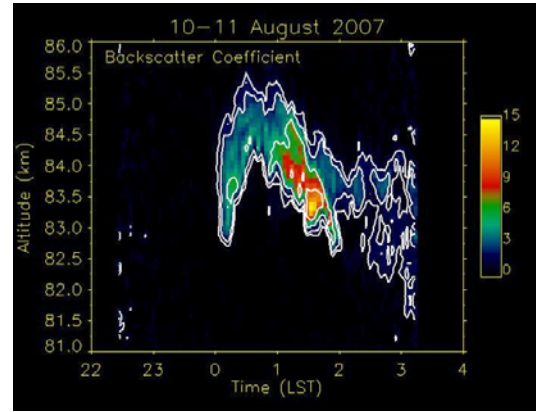


Figure 7 Lidar data showing an NLC profile from the Rayleigh lidar located at the Poker Flat Research Range just north of Fairbanks, AK. Courtesy Richard Collins, University of Alaska, Fairbanks.

2.4. Radar

Radar, instead of detecting the NLC ice particles directly, detects a related phenomena referred to as Polar Mesospheric Summer Echoes (PMSE). These phenomena are intense coherent radar echoes which were first observed in the late 1970s (Czechowsky et al, 1979). PMSE occur immediately above and sometimes overlapping the NLC layer and the two are linked together usually by different parts of the ice particle spectrum with the PMSE being highly sensitive smaller subvisual particles. Radar detection of PMSE also depends on the background ionospheric parameters such as the electron density and to neutral motions and turbulence (Rapp and Lübken, 2004). Using radar, information on the altitude, structure, annual variation, and winds can be

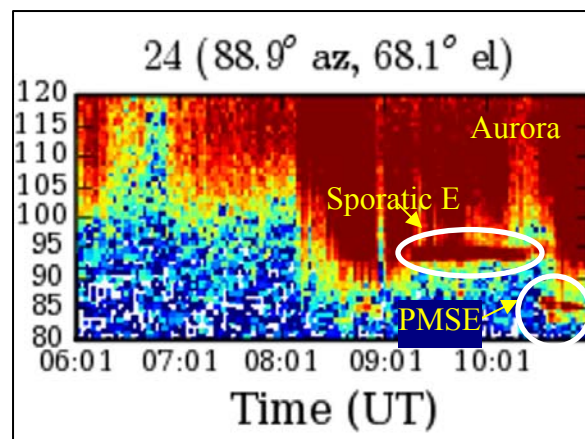


Figure 8 An example of Radar data from PFISR, incoherent scatter radar located at the Poker Flat Research Range. Courtesy Craig Heinselman, SRI

gathered. One important aspect of radar measurements is that the network of radars in both the northern and southern hemispheres is extensive, creating a large, data set on PMSE which can then be compared to the data collected on NLC using other instruments such as lidar and optical instruments.

An example of radar data on PMSE which was collected on August 10/11, 2007 can be seen in Figure 8. In this plot a sporadic E layer is seen at ~95 km with intermittent PMSE at ~83-85 km. The aurora is also seen as vertical structure from ~90-120 km.

For the purpose of this investigation, ground-based optical measurements, and satellite measurements have been used to determine whether the data collected on NLC from below and PMC from above show common properties for coincident measurements.

3. Satellite Measurements of PMC

Over the past three decades satellite instruments have become increasingly important to studies of NLC/PMC. The first satellites to detect PMC were the OGO-6 satellite (Donahue et al., 1972) and the Solar Mesosphere Explorer (SME) Satellite (Thomas 1984). Since those early satellites there has been a continuous presence of instruments in space which have been capable of PMC investigations (although they were not specifically designed for this). These include the NOAA satellite suite which has provided over 30 years of continuous data. Satellite instruments are able to take measurements of the clouds during full daylight which is especially important at high (polar) latitudes where the sun never gets low enough to allow viewing NLC from the ground. These studies have culminated in the recent launch of the Aeronomy of Ice in the Mesosphere (AIM) Satellite, which is the first satellite designed specifically to study PMC, in 2007. For this investigation we have focused on three available sets of satellite data. The instruments used in this comparison are the Solar Backscatter Ultra Violet (SBUV/2) instruments on the NOAA weather satellites, the Ozone Monitoring Instrument (OMI) on the AURA satellite, and the Cloud Imaging and Particle Size (CIPS) instrument on the AIM satellite.



Figure 10 NLC photographed by the Expedition 17 crew on the International Space Station on July 22, 2008 when the station was located ~340 km over western Mongolia. Courtesy NASA.

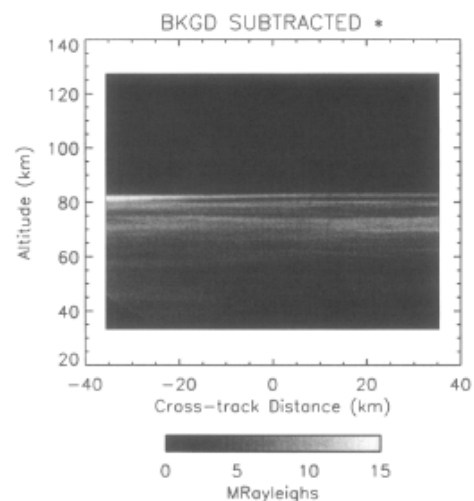


Figure 9 A typical background-corrected picture of polar mesospheric clouds observed by an ultraviolet imager on the MSX Satellite. (Carbary et al. 2003)

3.1. Solar Backscatter Ultraviolet (SBUV/2) Instruments

The NOAA satellites, are in sun-synchronous orbits at an altitude of ~ 850 km. The SBUV/2 instruments are nadir pointing non-spatial scanning instruments, which are primarily used to measure the abundance of stratospheric ozone. The SBUV/2 field of view is $\sim 150 \times 150$ km. SBUV/2 instruments have proven capable of detecting PMCs which appear in the data as spectrally dependent enhancements of the backscattered signal (e.g. DeLand et al., 2003). One of the key reasons these instruments are important in the study of PMCs is that nearly identical SBUV instruments have been in orbit since the mid 70's starting with the Nimbus-9 SBUV in 1978. Since that first satellite, there has been at least one, and usually two or three, SBUV instruments operational. This has resulted in nearly 30 years of continuous data on PMC brightness and occurrence frequency. As such, these instruments offer invaluable information concerning changes in the clouds over the past three decades. An example of the PMC data collected by one of the SBUV/2 instruments can be seen in Figure 11. Thomas (2003) defined the 'residual' PMC albedo, the intensity of the light scattered off the clouds, as radiance/solar irradiance and the residuals due to PMCs are typically $\leq 10\%$ of the background. This means that only the brighter PMCs can be separated from the ozone background. This is

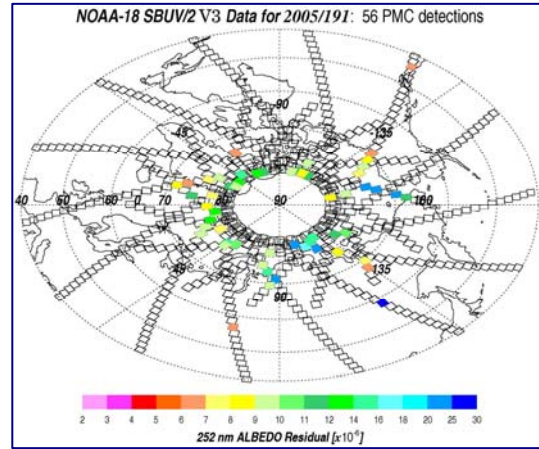


Figure 11 Summary PMC data collected from the SBUV/2 instrument on the NOAA 18 satellite. The boxes indicate the spatial extent of each scan and the fill color indicates the residual albedo of a PMC detection.

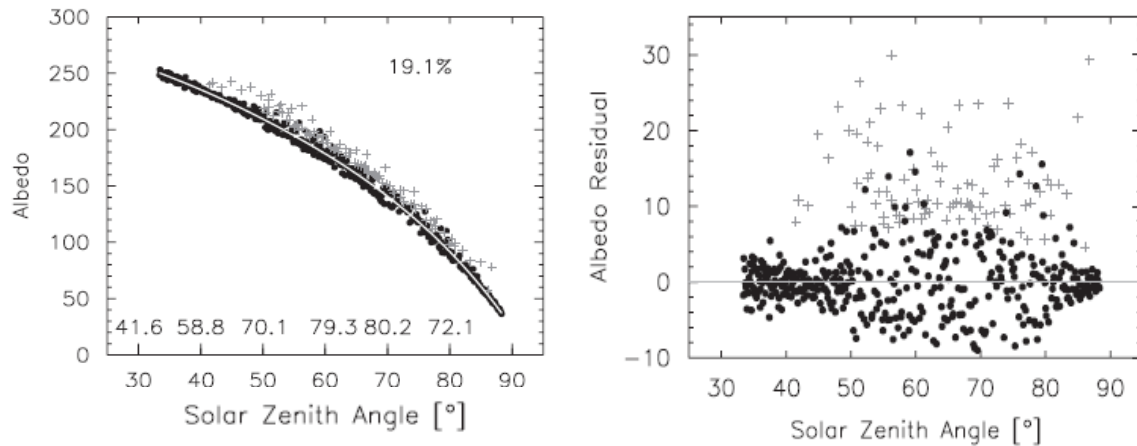


Figure 12 Comparison of the albedo (left) and albedo residual (right) derived from the SBUV/2 cloud detection algorithm as a function of solar zenith angle for the NOAA-17 SBUV/2 data from 20 July 2007. Albedo and albedo residual units on all plots are 10^{-6} sr^{-1} . Black, closed circles denote non-cloud points; gray, plus symbols represent cloud detections. (the latitude range is indicated in the left panel.) The white line in the left panels indicates a fourth order polynomial fit to the background enabling the residuals to be determined. (Benze et al. 2008).

illustrated in figure 12. Thomas (2003) also defines the frequency of occurrence as the number of PMC detections divided by the total number of observations from 50° to 82.5° and from June 2 to August 6.

The SBUV/2 detection algorithm consists of several tests which compare the residual albedo at various wavelengths to determine whether or not each observation is a viable PMC detection. The first test requires that the residual albedo is positive at the three shortest wavelengths. The second test requires a negative slope for a linear regression fit to the residuals measured at each of the five wavelengths. This negative value comes from the fact that the PMC scattering should be stronger for shorter wavelengths. The third test looks at the ratio of the residuals at 252 nm to 273 nm. For a PMC detection this ratio should be >1. The final test checks that the residual is higher than either the absolute or relative threshold (whichever is the smaller of the two values). The absolute threshold is $7 \times 10^{-6} \text{ sr}^{-1}$ and the relative threshold is 1.05 times the average background. These tests are run five times after which all points not flagged as PMC detections in any of the iterations are determined to be background (e.g. DeLand et al. 2007). If a measurement passes all of these tests it is flagged as a PMC detection and if it passes all but one of the tests it is flagged as a faint detection. It is questionable whether these points correspond to actual PMCs but when they occur next to PMC detections they are often incorporated into the list of detections to give a more complete look at the clouds. These points are also useful in comparing the SBUV/2 data with data from ground-based measurements or from other satellites. The results of these tests for the data from July 20, 2007 can be seen in Figure 12.

3.2. Ozone Monitoring Instrument (OMI)

OMI is a primary instrument on the AURA satellite which, like SBUV/2, was designed to mainly study stratospheric ozone. A NASA proposal to utilize AURA science data to study PMC with data from OMI was recently funded and Utah State University is participating in this program. OMI was designed to study aerosols and investigate total ozone by observing solar backscatter radiation using a hyper-spectral imager monitoring wavelengths from 270 to 500nm. Rather than taking data only in nadir, OMI takes data in ‘swaths’ that span $\sim \pm 61^\circ$ from the nadir dramatically increasing the spatial coverage of the instrument compared to that of SBUV/2. Although it was designed to study ozone, OMI is capable of detecting PMCs in the same way as the SBUV/2 instruments but with higher sensitivity and spatial resolution so a more detailed study of the spatial occurrence and frequency of these clouds is possible. Measurements are extracted from this data through a series of algorithms, similar to those described above for the SBUV/2 instruments, which strip off the ozone signal and determine whether the residual backscatter signals are high enough and at the right wavelengths (around 273 nm) to

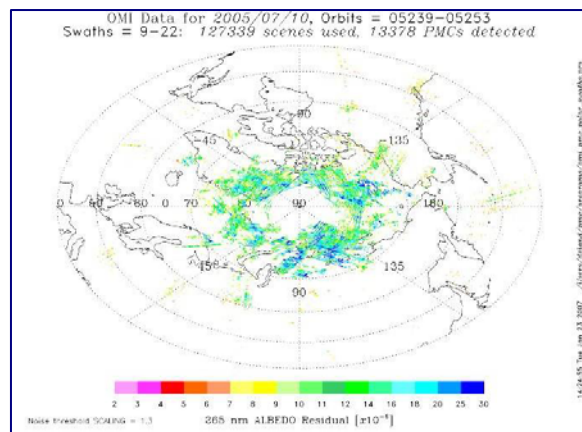


Figure 13 An example of PMC data collected by the Ozone Monitoring Instrument for a 24 hour period on July 10, 2005.

have originated from PMCs. An example of the PMC data from OMI derived from OMI can be seen in Figure 13. Due to its increased sensitivity, OMI has more capability of detecting PMC at latitudes $\leq 50^\circ$ and therefore offers more opportunities for comparisons between lower latitude NLC and satellite detections of PMC. At NLC latitudes, SBUV/2 has difficulty detecting clouds due to the fact that they are faint and when the backscatter signal is averaged over the large field of view (~ 150 km) the cloud is lost in the background.

The detection algorithm for OMI consists of several tests which the gathered signals from the various wavelengths must pass in order to be flagged as a PMC. These tests are similar to those described above for the SBUV/2 instruments but must also take into account the scanning ability of OMI, making adjustments for measurements made off-nadir. If the signal passes all but one or two of these tests, the observation is tagged as a possible faint detection. The faint detections which are near definite PMC detections are incorporated into the overall data set to give a better picture of the possible PMC coverage. However, the PMC detection algorithm for this instrument is still in its preliminary stages of development.

3.3. Aeronomy of Ice in the Mesosphere (AIM)

The AIM satellite is a two year mission designed specifically to study PMC. The primary goal is to quantify how PMCs form, and to investigate their temporal and spatial variability. AIM was successfully launched on the 25th of April 2007 into a 600 km circular, sun-synchronous orbit. The principle investigator of this mission is Dr. James Russell III of Hampton University. There are three key instruments on the AIM satellite; CIPS, SOFIE and CDE.

CIPS (Cloud Imaging and Particle Size) is a UV imager comprising four cameras, two nadir one front and one aft, and is designed to provide images of PMC as the spacecraft flies over the polar region. CIPS has a field of view of ~ 2000 by 1000 km with 2 km horizontal resolution and operates at a 265 nm centered wavelength, similar to that used by SBUV/2. This instrument has provided the first detailed look at PMC structure from

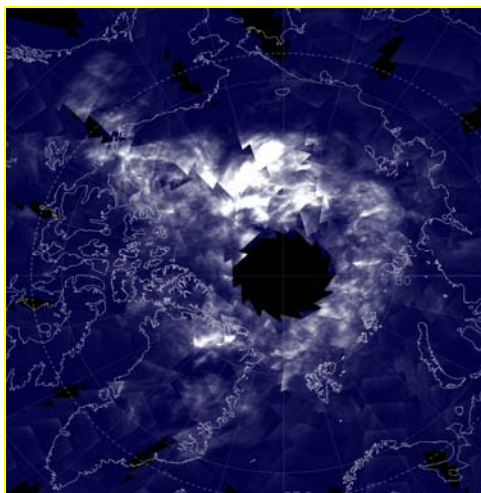


Figure 14 A 24 hour summary “daisy” plot from the CIPS instrument. July 5, 2007.

space. The data collected by CIPS is currently being used to study the wave formations in the clouds as well as to look at particle sizes, occurrence frequency, and brightness. A 24 hour

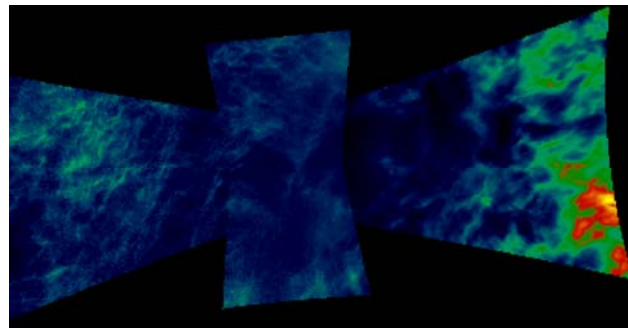


Figure 15 An individual scene from the CIPS UV imager on the AIM satellite. Color variations indicate the intensity of the light scattered by the clouds.

summary plot illustrating PMC variability over the north polar region can be seen in Figure 14.

SOFIE (Solar Occultation for Ice Experiment) uses solar occultation techniques to measure absorption in 8 spectral bands from 0.25 μ m to 6.0 μ m from five gaseous species (H₂O, CO₂, O₃, CH₄, NO) with a 2 km vertical resolution. This instrument is also designed to take a temperature profile from the troposphere to the lower thermosphere.

CDE is the Cosmic Dust Experiment and is designed to determine how much dust is present in the upper atmosphere. This is important because the prominent theory on NLC formation is that water vapor in the mesopause region nucleates on cosmic dust to form the microscopic cloud particles (typically <60 nm). (Gadsden and Schröder, 1989)

4. Ground-Based NLC Campaigns

The study of NLC was pioneered by ground-based measurements. Matching satellite data with image data taken from the ground is important but due to observational constraints the instruments tend to see different parts of the summer mesopause region. Comparing the data sets between satellite and ground can also give a much clearer picture of the extensive properties of NLC/PMC. In order to collect ground-based measurements of NLC for comparison with measurements by the newly launched AIM satellite, we conducted two field campaigns from Canada and Alaska during the summer of 2007. A separate goal of these campaigns was to collect data from two sites in order to build a stereo map of the cloud structures.

4.1. Canada (June 31-July 14, 2007)

The primary goal for this campaign was to perform two-station imaging of NLC from Edmonton, AB, which is ideally situated for NLC twilight studies. The primary sites used during this campaign were Namao (53.7°N, 113.5°W), and Beaver Creek (53.75°N, 112.7°W), and Lamont (53.8°N, 112.8°W) for one night. Image data were collected by C.D. Burton, USU, and M. Zalcik, the Canadian Amateur NLC Network (CanAM) Coordinator. During the 15 day campaign NLC were observed and photographed on no less than eight of eleven clear nights with a 78% occurrence frequency. The instruments

Summary:	LT = UT – 6 hrs
6/30 - 7/01 Faint NLC 00:25 - 03:36 LT	
7/1 - 7/2 NLC visible from 23:48 LT to dawn at 04:03 LT	
7/3 - 7/4 Limited NLC from 23:42 – 01:45 LT	
7/4 – 7/5 Bright NLC from 23:28 – 03:14 LT (cloud later)	
7/5 – 7/6 Faint NLC 22:53 – 23:19 LT (Storm stopped observations)	
7/7 – 7/8 Faint NLC from 01:30 – 03:40 LT (condensation later)	
7/12 – 7/13 Faint NLC 02:00 – 03:10 LT	
7/13 – 7/14 Limited low elevation NLC 11:46 – 03:54 LT	
Total 8 NLC displays observed on 11 clear nights (78%)	

Table 1 A summary of the nights for which data were collected during the Campaign in Canada during the summer of 2007.



Figure 16 A Stereo Image Pair taken on July 5 2007 at 05:49:28 UT from Namao and Beaver Creek in Alberta, Canada.

used during this campaign were two Canon 30d digital cameras with fields of view of $\sim 30^\circ V \times 40^\circ H$. The cameras were controlled by Dell Inspiron laptops which were synchronized before data were collected and the cameras were set to take pictures every 30 seconds starting on the minute in order to ensure that the images matched temporally. The data from these eight NLC nights are summarized in Table 1. On each occasion Twilight observations lasted for ~ 4 hr. At each site, the cameras were directed due north using the star field and set at a central elevation of 15° to ensure that the same structures were being imaged. An example of the two station imaging can be seen in Figure 16. The site separation was ~ 50 km for the images.

4.2. Alaska (June 23-August 18, 2007)

For this campaign, the primary goal was to collect measurements of NLC dynamics with several instruments in coordination with AIM overpasses. The instruments used were the Iron Lidar, Rayleigh Lidar and Incoherent Scatter Radar (PFISR) located at Poker Flat Research Range (PFRR) ($65^\circ N$, $147.5^\circ W$) just north of Fairbanks, AK, along with two-station color CCD imaging.

The two sites used for imaging were located at Donnelley Dome ($63.8^\circ N$, $145.8^\circ W$) and Gristle River ($63.8^\circ N$, $144.9^\circ W$). The Donnelley Dome site was run by C.D. Burton while the Gristle River Site was run by J. Barker-Tvedtnes, both from USU. These locations were separated by ~ 43 km and the ground range to PFRR was ~ 166.5 km for the Donnelley Dome site and ~ 189 km for the Gristle River site. The cameras were oriented to $\sim 35^\circ W$ of N and 15° elevation in order to image the cloud structures over the lidar and radar. The PFRR elevation was $\sim 27^\circ$ assuming an NLC layer at 83 km. The site geometry can be seen in Figure 17. The instruments used during the campaign were identical to those used during the Canadian



Figure 17 The site geometry for the NLC campaign in Alaska. (Courtesy Google) Images were being taken of the same cloud structures which were recorded by the lidar and radar at PFRR.

Campaign. A video camera was also used at each site to collect additional data on the dynamics of the display.

During the 24 day campaign data were collected on only three nights due to poor weather conditions. On July 26/27 photographs were taken from the UAF campus for ~0.5 hr from 10:00 to 10:30 UT (2:00-2:30 LT). On the night of August 10/11 images were collected from both sites described above of a bright NLC display for ~4 hrs from 8:30 to 12:30 UT (12:30-04:30 LT). On the following night NLC were again detected, but through cloud. The 10/11 display was also recorded by the radar and both lidars at PFRR as well as during an overpass of the AIM satellite at 9:00 UT (1:00 Alaska Daylight Time). An example of the two station image data from this night can be seen in Figure 18 where the parallax in the cloud structures between the two sites is indicated by the arrows.

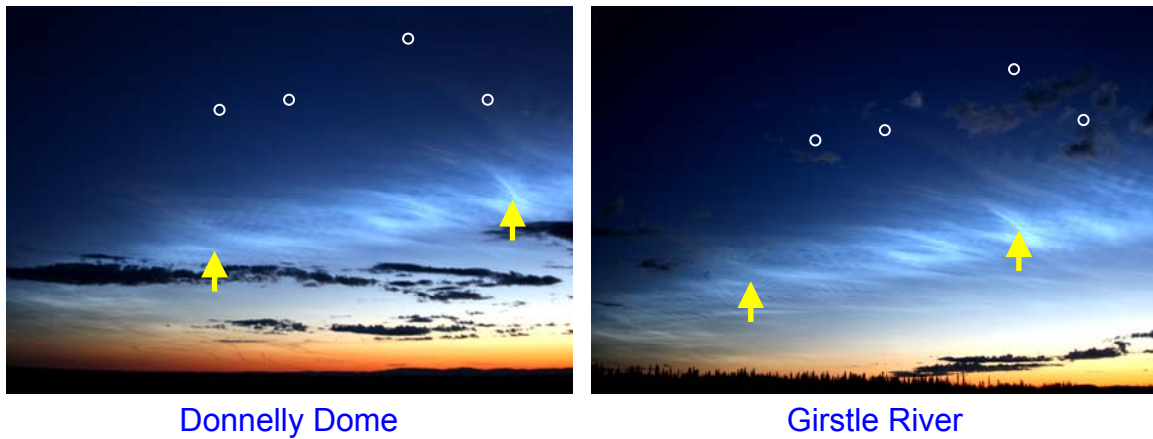


Figure 18 An example of the NLC data collected during the campaign in Alaska. The images are from the night of August 10/11 and the parallax between the two sites is indicated by the arrows. The circles indicate the common star field in each image.

5. Analysis and Results

5.1. Ground-Based Data Analysis

Following the campaigns the data collected were compiled and analyzed to determine the

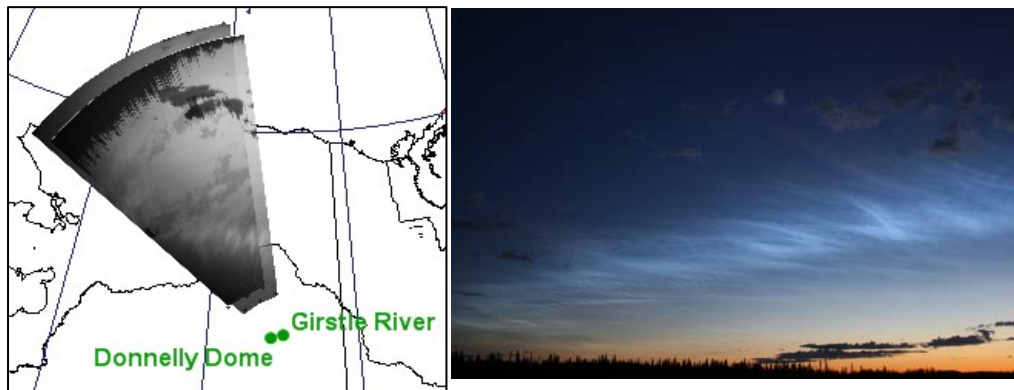


Figure 19 (Left) Two-station images of an NLC un-warped and projected onto a geographic map. The images were taken on August 10/11 at 2:00 LT from Donnelly Dome and the Girstle River. (Right) The original image of the NLC taken from the site on the Girstle River.

geographic locations of the cloud formations. This was done using a program developed at USU in the Center for Atmospheric and Space Science (CASS). The program uses the star field present in the images along with an assumed cloud height of 83 km to un-warp them so they can be placed over a geographic map. This shows the location of the clouds and allows for a comparison with corresponding satellite and ground-based data. These images also give an idea of how the structures would look if you were standing directly below them and can be used to determine the wavelength of the various periodic structures in the NLC. In addition, the images were collected to create a time lapse view of the dynamics of the display throughout the night from each site. An example of the analyzed data from Aug. 10/11, 2007 can be seen in Figure 19.

5.2. Satellite Comparisons

In order to compare satellite data sets it is necessary to determine how well the data collected by the different instruments agrees. What follows are comparative studies between OMI and SBUV/2 and between AIM and SBUV/2. Three days were selected for an initial comparison between AIM / SBUV/2 and OMI / SBUV/2. These days were selected based on the amount of PMC activity as determined from AIM imagery and are as follows: Day 190 (moderate), day 200 (high), and day 223 (low) PMC activity.

5.2.1. Comparison of OMI and SBUV/2

Comparing OMI and the SBUV/2 instruments can be accomplished by simply mapping the two data sets together and determining how often the SBUV/2 PMC detections correspond to OMI PMC detections. The reason the comparison can be carried out in this

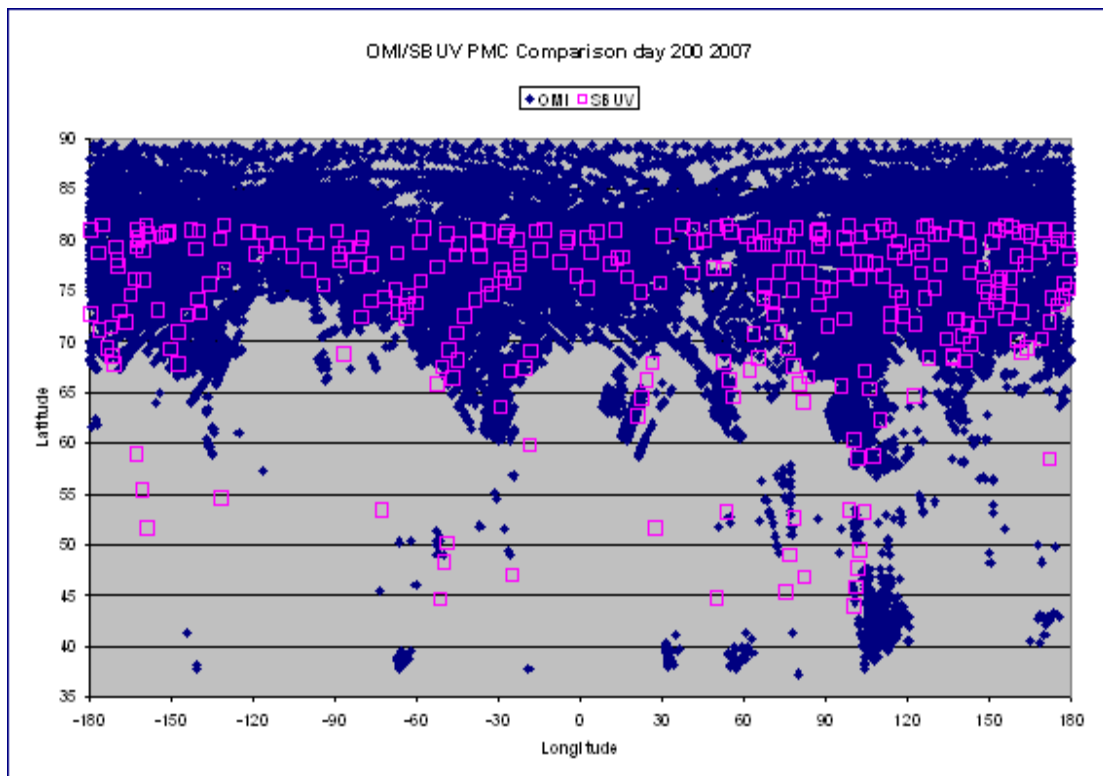


Figure 20 Comparison of SBUV and OMI data for a 24 hour period (day 200). The open boxes indicate SBUV/2 PMC detections while the diamonds indicate OMI PMC detections.

fashion is that the instruments are very similar in the way they make measurements of the atmosphere and because they were both designed to study atmospheric ozone so the algorithms for determining whether measurements are PMC detections are already compatible. For the three days investigated in the OMI / SBUV/2 spatial comparison with limited 24 hour temporal comparison shows agreement of ~94% for day 190, ~95% for day 200 and ~88% for day 223. The spatial comparison for day 200 can be seen in Figure 20. In this figure we see a much greater number of PMC detections from OMI than from SBUV (as expected) and the data comparison is not as good at lower latitudes where SBUV is less sensitive. From this initial study, we see that the agreement is greater for the days with active and moderate PMC activity than for the day with little PMC activity. This conclusion agrees well with the AIM / SBUV/2 comparison for these three days (described below). This is an ongoing study.

5.2.2. AIM and SBUV/2

In order to compare AIM, SBUV/2, and ground-based data it is important to know how the satellite data sets match up with each other. To this end, the same three days (190, 200, 223) were compared for the AIM and SBUV/2 instruments to determine the correlation between the data sets. Because the resolution of AIM is much higher than that of SBUV/2 the AIM data were averaged to that of the SBUV ‘footprint’ (150 x 150 km). IN a recent study by Benze et al (2008) a comparison between AIM and SBUV/2 data was presented using a revised algorithm which was designed to work on both data sets, but which neglected the spectral variation in the SBUV/2 data and the spatial resolution of the CIPS instrument. Basically, the study compared SBUV/2 at 273 nm with AIM at 265 nm. These wavelengths were chosen due to the fact that no correction was necessary so the data could be compared directly. These conditions allowed a direct comparison of the two data sets because they removed the need to account for differences in the data collection. The results of this particular study served as a validation of the AIM data since it was found that the SBUV/2 and AIM data agreed to within ~10% over the entire summer season. This comparison also served to link the two data sets so that AIM data can be used to carry on the statistical data set created by over 30 years of SBUV data. Another aspect of the comparison was to look at a day with no PMC activity to compare the background of the two data sets. Again the two instruments showed very good agreement (Benze et al, 2008).

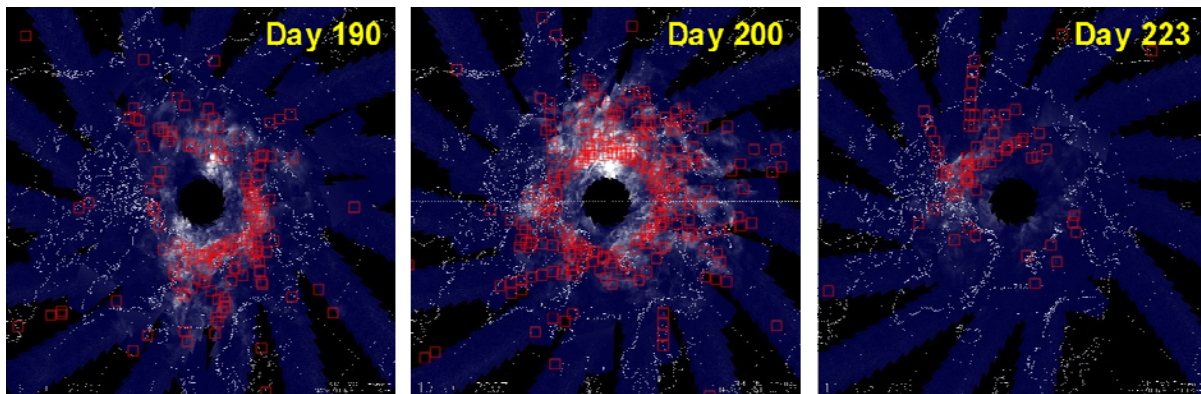


Figure 21 Comparison ‘daisy’ plots for day 190, 200, and 223. The SBUV data are seen as open boxes over the AIM ‘daisy’ for each 24-hour period.

For our purposes we have used a direct one to one comparison of the data sets from the two satellites for the three example days during the 2007 Northern Hemisphere season. The full detection algorithms were used in order to take advantage of the full capability of each satellite to determine whether the two instruments were ‘seeing’ the same clouds.

These specific days were chosen based on the amount of PMC activity. Day 200 shows a high amount of PMC activity down to latitudes of $\sim 45^\circ$, day 190 shows moderate PMC activity and day 223 shows very little activity which is confined mostly to latitudes above 60° . The purpose of this comparison was to determine whether the two satellite instruments showed more agreement on days with high PMC occurrence than days with little activity. For this comparison, SBUV/2 data were compared first temporally with AIM orbits then mapped together to determine whether any of the data were spatially coincident. The criterion for temporal coincidence was that the SBUV/2 data must fall within ± 1 hour centered on the AIM orbit in question. Spatial coincidence was determined visually and required that the SBUV/2 detection must lie within the AIM orbit swath (~ 1000 wide). This criterion removes some of the ambiguities in the comparison due to spatial variability of the PMCs. By mapping all of the SBUV/2 measurements, both detections and non-detections, with the temporally coincident AIM orbit it is possible to determine a percentage for the agreement between the two data sets. Initially, mapping the SBUV/2 detections for each day with the corresponding AIM ‘daisy plot’, a daily summary plot which uses shows all of the data collected by the front camera on the CIPS instrument during a 24 hour period, shows generally good agreement between the data sets, as expected. The ‘daisy comparison’ for each day can be seen in Figure 21. The AIM data used for this detailed comparison was version 3.12, level 4a, which has a resolution of ~ 15 km. The original analysis was carried out using an IDL program developed by the CIPS team at the Laboratory for Atmospheric and Space Physics in Boulder, Colorado, and shows the individual orbits over a geographic map.

Separate data comparisons were conducted for these three days. Only comparing SBUV/2 PMC detections revealed that the data agree to within 5%, 2%, and 8% for days 190, 200, and 223 respectively. The results for this comparison one-to-one are slightly better than the 10% statistical result reported by Benze et al. (2008) using the modified detection algorithms for the two data sets and the NOAA-17 SBUV/2 instrument. It is evident that day 200 shows better agreement between the two instruments but correlation on the weak PMC day (223) still shows agreement for over 90% of the time. However, comparing all coincident SBUV/2 measurements, detections and non-detections, gave less favorable results of $\sim 63\%$ agreement. This result may be improved by taking into account the ‘faint’ SBUV/2 PMC detections which are measurements which passed some of the tests for PMC detections but failed others. Examples of the compared data using individual AIM orbits can be seen in Figure 22.

When considering non-detections only, the agreement for the three days was 47%, 47%, and 65% for day 190, 200, and 223 respectively. These results show that 53% of the time that SBUV/2 measurement detected no PMC, AIM did detect the clouds on both the active and moderate days. For the day with light PMC activity this number drops to 35%. Overall the CIPS instrument is $\sim 50\%$ more sensitive than the SBUV/2 instruments for PMC detection (which is to be expected since AIM was designed to study PMC whereas SBUV/2 was not). Again, taking into account the faint detections in the SBUV/2 data set

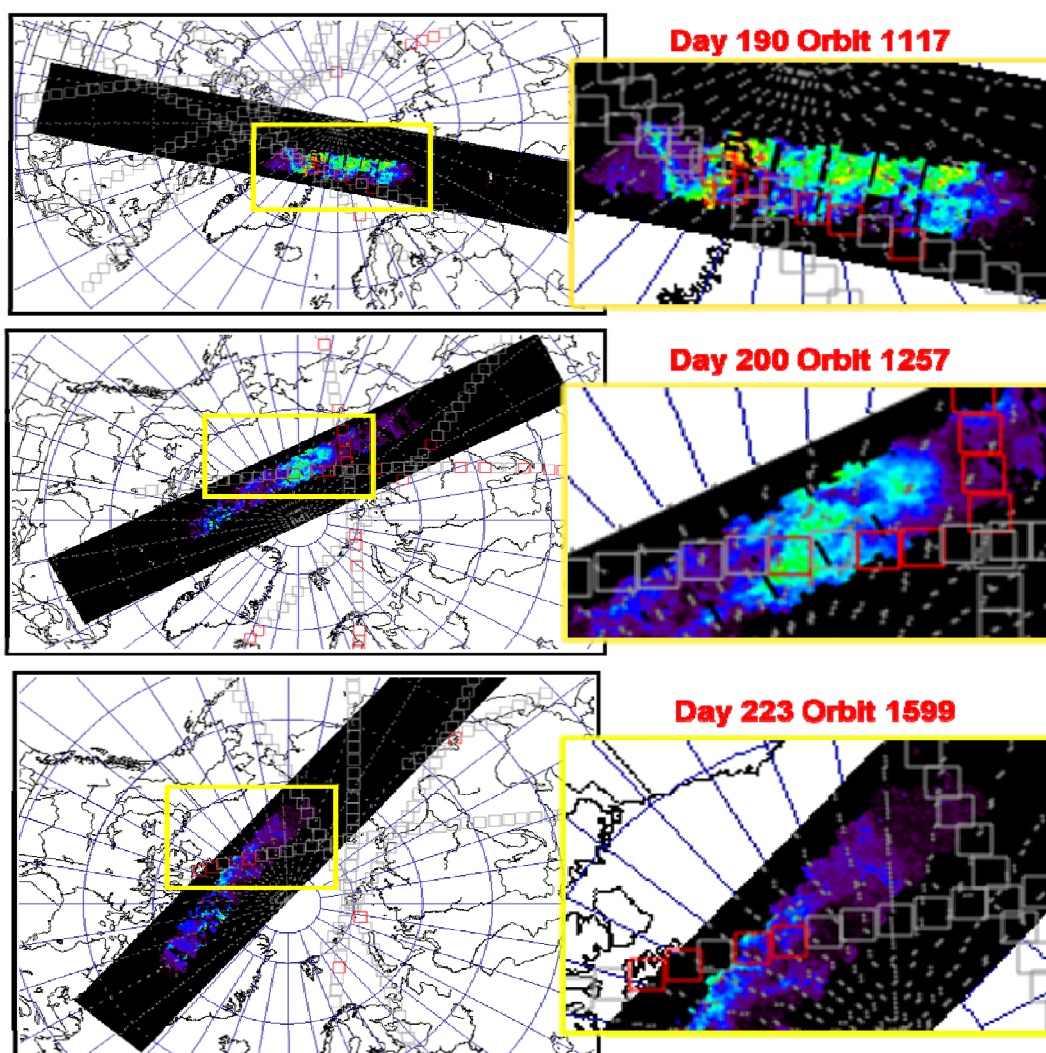


Figure 22 Example data from the comparison using individual AIM orbits and the corresponding SBUV measurements. The images on the right are enlargements of the data in the yellow boxes in the images on the left. Each of these orbits shows excellent agreement between the SBUV PMC detections and the AIM PMC data.

day	PMC activity	% detection agreement	% non-det agreement	% total agreement
190	moderate	95	47	0.57
200	active	98	47	0.61
223	mild	92	65	0.67

Table 2 The results for the AIM / SBUV/2 comparison for days 190, 200, and 223 during the 2007 NLC season.

5.3. Satellite and Ground-Based Data

For this comparison study there were several SBUV/2 instruments. Since these instruments are nearly identical, it is unimportant which satellite made the individual measurements. When comparing SBUV/2 with ground-based measurements the criterion

for coincident data is that the satellite detection occurred within ± 4 hr and $\pm 20^\circ$ longitude and 5° latitude of the ground-based measurement.

Our comparison with AIM data was restricted to the Alaskan data set due to the fact that AIM was not designed to see PMC at latitudes typically less than 60° and so it does not allow for a comparison with the Canadian data. The criterion for coincidence was the same as that set for the SBUV/2 study.

For coincidence between OMI and ground-based measurement, the criterion was that the OMI detections fall within a 200 km radius of the ground-based site. For the Canadian data this corresponds to $\sim 2^\circ$ latitude and 3° longitude and for the Alaskan data this is $\sim 2^\circ$ latitude and 4° longitude centered about the site.

5.3.1. Canadian Comparison

From the Canadian campaign, using the parameters above, the nights of July 1/2, 3/4, and 4/5 showed coincidence between SBUV/2 and ground-based data. There was also coincidence with a 5° or greater latitudinal gap for the nights of the 7/8 and the 12/13.

July 1/2, 2007

For the night of July 1/2, 2007 (Day 183), the SBUV/2 data extended directly over the imaging sites, but ~ 2 hrs after the clouds were no longer visible from the ground due to dawn. No clouds were detected during the previous or following orbits in this area. Figure 23 shows a ground-based image mapped together with the satellite detections ~ 2.5 hours later. The excellent spatial coincidence of these data suggest that the clouds were still present in the area for at least 2 hours after they were no longer visible from the ground.

OMI data for this night also show one PMC detection within a 200 km radius centered on the Edmonton region, but with a fairly low albedo of $\sim 6 \times 10^{-6} \text{SR}^{-1}$ at 287nm. This data can be seen in Figure 24.

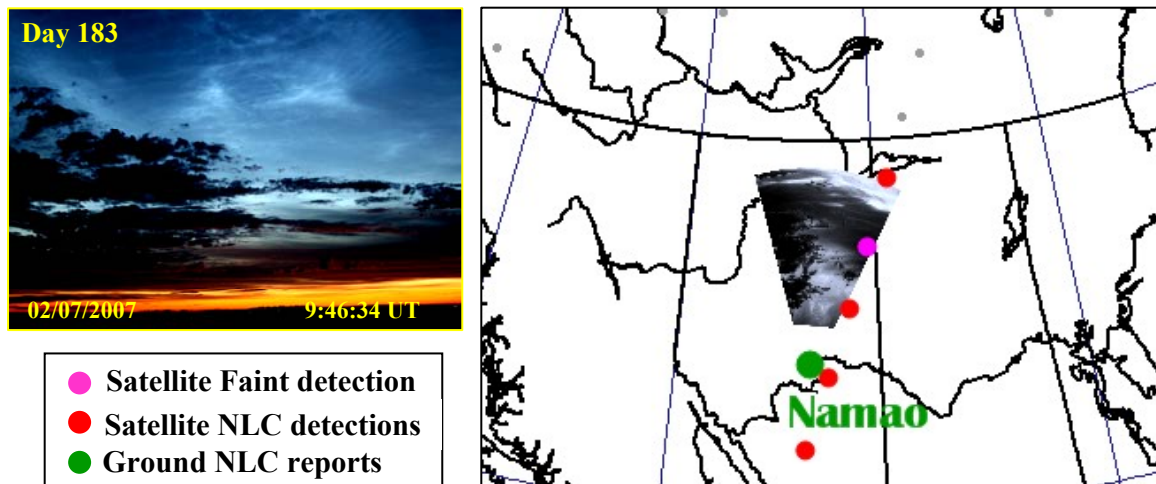


Figure 23 Data collected on the night of July 1/2 2007. Right: The SBUV data, shown by the red and pink dots, extends directly over the imaging sites ~ 2 hrs after imaging ceased. Left: NLC image taken at 9:46 UT from Namao by Mark Zalcik (CanAM Coordinator)

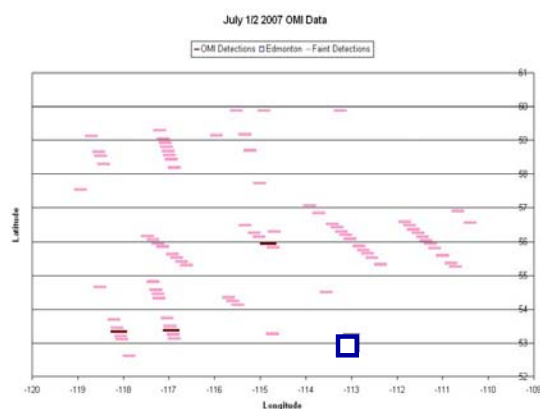


Figure 24 OMI data for day 183. The box indicates the location of Edmonton Canada, the light lines indicate faint PMC detections and the dark lines indicate strong PMC detections over a range of 10° in both latitude and longitude.

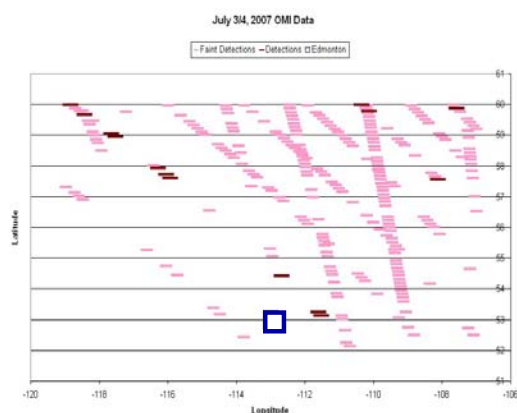


Figure 25 OMI Data for day 185. The box indicates the location of Edmonton Canada, the light lines are faint PMC detections and the dark lines indicate strong PMC detections.

July 3/4, 2007

The 3/4 of July (Day 185) gave coincident data with small gaps between the SBUV/2 and ground-based data sets both spatially and temporally. SBUV/2 data from an overpass ~ 1.5 hours before imaging began lay $\sim 3^\circ$ north of the imaging site (data not shown). There were also PMC detections $\sim 10^\circ$ west for a separate SBUV/2 overpass ~ 2 hours after the NLC were no longer visible from the ground.

OMI data for this night showed three coincident detections with albedo of $\sim 7.5 \times 10^{-6} \text{SR}^{-1}$ at 287nm. This data is plotted along with the ground-based sites in Figure 25.

July 4/5, 2007

For the night of July 4/5, 2007 (Day 186) satellite NLC detections were present $\sim 10^\circ$ west of the camera sites and were temporally coincident with the ground-based data. There were also detections $\sim 5^\circ$ north of the sites and ~ 1.5 hr before the NLC was visible

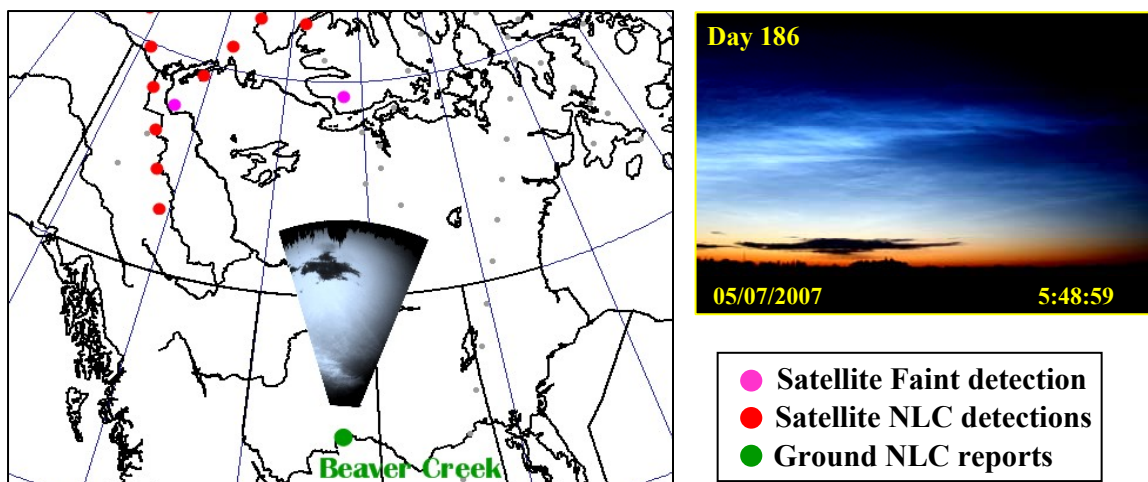


Figure 26 Data collected for the night of the 4/5 of July. Left: The un-warped ground-based image mapped with temporally coincident SBUV/2 detections. Right: NLC image taken at 5:49 UT from Namao, Canada by Mark Zalcik.

from the ground. This implies that the display was far more extensive than the ground-based images were able to reveal with the clouds extending to both the north and west. This data can be seen in Figure 26. There were also reports from two locations to the west of Edmonton which observed NLC displays on this night. These reports came from the CanAM NLC viewing network which is an amateur viewing network throughout Canada and the Northern United States. The reports were collected and compiled by Mark Zalcik, of Edmonton, Canada. Unfortunately there were no coincident OMI data available for this event.

5.3.2. Alaskan Comparison

For the ground-based data collected during the NLC display on the 10/11 of August there was coincidence data available from the AIM satellite, two NOAA satellites, and OMI. This night offers our most comprehensive look at how the data sets can differ between ground-based and satellite measurements.

Looking at the available SBUV/2 data we see that NOAA 18 passed over from 13:56 to 13:58 UT, but 1.5 hrs after ground observations stopped due to dawn. During this overpass the satellite detected PMCs over Alaska, from ~ 75 to 70°N . The following overpass at 14:35 had detections over western Canada from ~ 75 to 63°N and 115 to 140°W . NOAA 16 passed over Alaska from 16:14 to 16:18 UT, 3.5 hrs after ground observations ceased. During this overpass the satellite detected PMCs from ~ 75 to 60°N . Both of these satellites generally gave good coincidence with the ground-based data. Figure 28 plots all of the SBUV/2 PMC detections within ± 4 hrs and 10° latitude mapped with the ground-based data from both sites to show the overlap in the data.

AIM passed over PFRR at 9:00 UT (1:00 LDT) while imaging was taking place giving perfect temporal agreement with the ground-based data. The spatial agreement was also very good but a small 1° spatial gap was determined between the ground and CIPS images. This unexpected gap is currently under investigation.

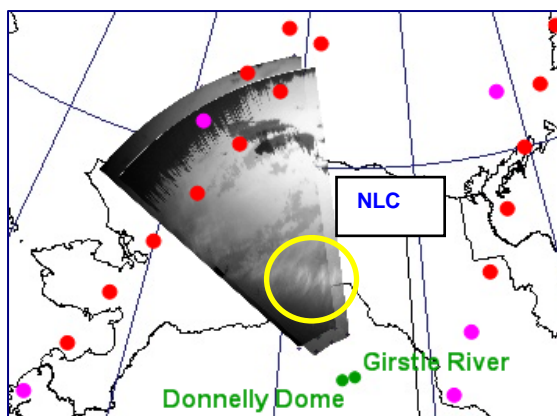


Figure 28 Two station images mapped with the coincident SBUV/2 detections for the night of August 10/11.

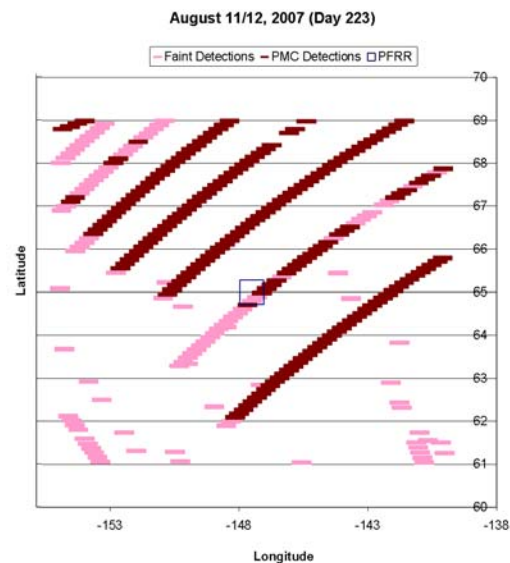


Figure 27 Spatially coincident OMI / ground-based data for August 10/11, 2007. The box indicates the location of PFRR, dark lines are PMC detections, light lines are faint detections.

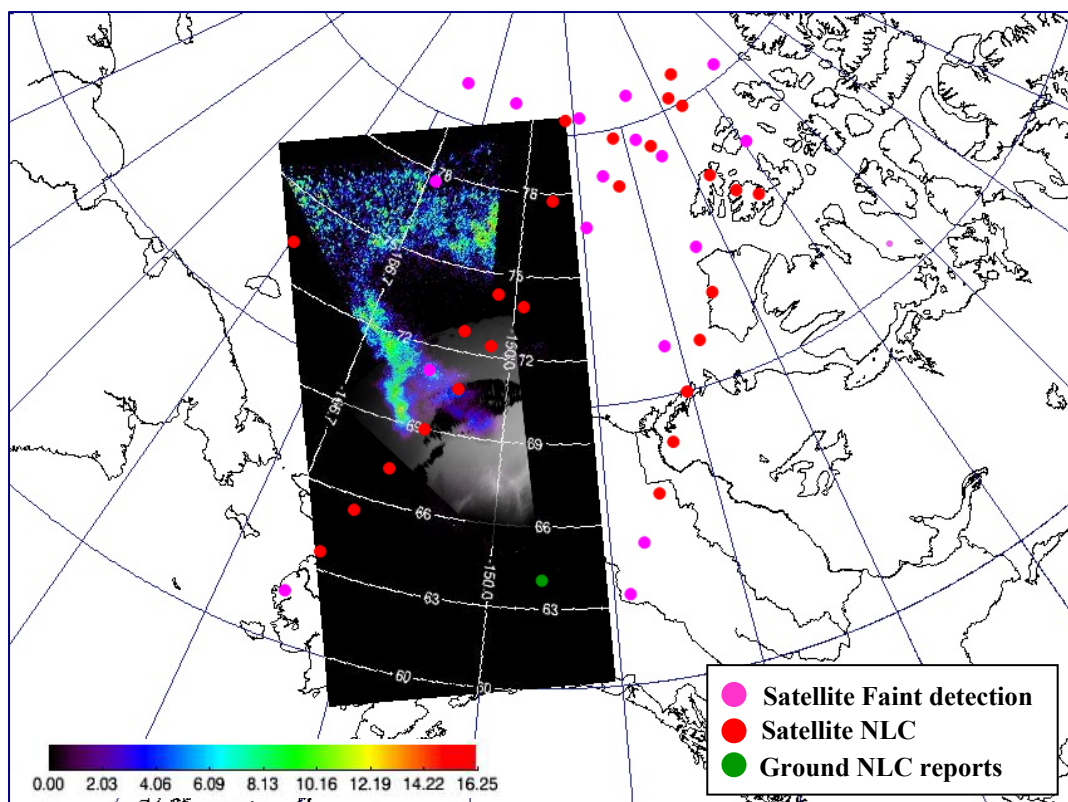


Figure 29 A data comparison for the night of the 10/11 of August 2007. The color bar indicates the intensity of the AIM PMC signal while the pink and red dots indicate SBUV detections from both the NOAA 16 and 18 Satellites. The ground-based NLC data has been un-warped to show the geographic location of the NLC display.

The SBUV/2, AIM, and ground-based data are shown together in Figure 29. This figure shows clear agreement between all three data sets and gives us a novel look at the NLC as they are seen both from above and from below. A comparison of the spatial features in the clouds is difficult due to the small spatial gap between CIPS and ground images. However, the projected mapping in figure 26 clearly show that the NLC captured by the ground-based images were only a small part of a much larger PMC display that extended well into the polar cap region.

OMI data for this event was also extensive with 51 detections within a 200 km radius centered on PFRR. The average albedo for the coincident measurements was $\sim 1 \times 10^{-5} \text{ sr}^{-1}$ significantly brighter than the other displays discussed herein. This combined data set is still under investigation and has the potential to connect the AIM, SBUV/2, and ground-based data sets more fully to give a comprehensive look at the NLC display. Coincident OMI data for this night is plotted in Figure 27.

6. Summary

The four nights investigated are summarized below:

Day	Ground data	SBUV/2 Satellite data	AIM Satellite data	OMI Satellite Data (200 km radius)
June 1/2 Day 183	05:48-10:03 UT Sites: Namao and Lamont Bright NLC visible at dawn	12:20:48-12:22:56 UT Spatial coincidence with ground based images.	NA	1 detection Albedo: $\sim 6 \times 10^{-6} \text{SR}^{-1}$ at 287nm.
June 3/4 Day 185	05:42-07:45 UT Sites: Namao and Beaver Creek Moderate NLC visible all night	04:27:32-04:29:08 UT $\sim 3^\circ$ north of ground based images.	NA	3 detections Albedo: $\sim 7.5 \times 10^{-6} \text{sr}^{-1}$ at 287nm
June 4/5 Day 186	05:28-09:14 UT Sites: Namao and Beaver Creek Bright NLC visible all night	05:44:20-05:48:36 UT $\sim 10^\circ$ west of ground based images. 04:05:08 UT $\sim 5^\circ$ north of ground based images.	NA	NA
August 10/11 Day 223	08:20-12:20 UT Moderate to bright display visible all night. Cloud cover until $\sim 9:30$ UT at Girstle River site and from $\sim 10:30$ UT until dawn at the Donnelly Dome site.	14:31:28-14:34:40 UT $\sim 5^\circ$ west of ground based images. 16:11:44-16:18:08 UT & 13:56:53-13:57:57 UT Spatial coincidence with ground based images.	08:59:07-09:03:25 UT Temporal coincidence. Clouds appear $\sim 1^\circ$ north of the cloud structures in the ground-based images.	51 detections Albedo: $\sim 1 \times 10^{-5} \text{sr}^{-1}$ at 287 nm

7. Conclusions

For the four nights of PMC/NLC data analyzed, the SBUV/2 data expanded the duration of the NLC by an average of 3 ± 1 hr after the ground imaging ceased (at dawn) and 1 ± 0.5 hr (at dusk) before the clouds were visible from the ground. Spatially the satellite data expanded the known area of the display by up to 10° to the north, east and/or west when temporally coincident data were available.

AIM / CIPS data clearly connected the lower latitude NLC image data with the extensive polar cap PMC measurements paving the way for future in depth investigations.

OMI studies are currently limited, but our investigations have shown that they will be very important for low-latitude PMC investigations. This is demonstrated by the recent chance coincident NLC observations from Logan UT (41°N) and Rexburg ID (43.5°N). Such data will be important for investigating latitudinal gaps in the PMC/NLC regions as they may act as a bridge between the existing data sets.

In general it was found that there was either good temporal or spatial agreement between the satellite and the ground-based data sets, but rarely both for each of the four nights analyzed. Due to the differences in the methods by which the NLC/PMC data were gathered from ground-based and satellite instruments, coordinated measurements are difficult but important for better understanding the geographic and local time variability of PMCs. It is evident that we are looking at the same phenomena but that the data

present different pieces of the puzzle. We need to study all of these pieces in order to gain a full understanding of these beautiful and mysterious clouds.

8. Future Research

8.1. Investigation of the 5-day wave in OMI data

Merkel et al. (2003) conducted an investigation on the influence of the 5-day planetary wave on PMC structure and formation using the Student Nitric Oxide Explorer (SNOE) satellite data. When using OMI data to plot PMC frequency versus longitude at given latitudes, we have found evidence of the 5-day wave. An example of this can be seen in Figure 30. A new investigation is currently underway to quantify this longitudinal variation.

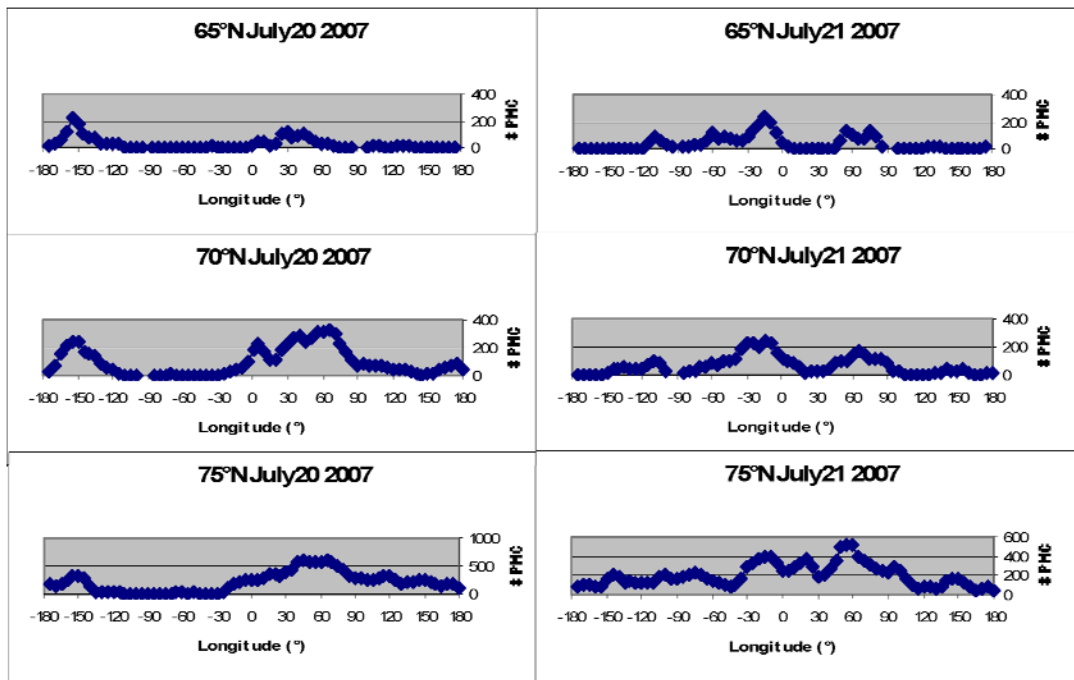


Figure 30 Examples of longitudinal variation and 70° N and 75° N in OMI PMC data for the nights of July 20 and 21 2007.

8.2. NEW OMI / AIM Global Study

A global comparison of OMI and AIM data similar to the one reported here for AIM and SBUV/2 will be conducted when the OMI PMC detection algorithm is completed. This comparison is expected to yield valuable information on the sensitivity of each of the instruments as well as connecting the low-latitude OMI data with the polar-latitude AIM data. This should also give more information on the unexpected gap in the AIM / ground-based comparison.

8.3. Investigation of the Gap

The fact that a gap existed between the AIM and ground-based data sets (for the one night of coincident data) is very mysterious, especially since the data were taken simultaneously and the same region was observed by each instrument. The reason for this gap is currently under investigation, but may be due to the different emission wavelengths utilized by CIPS (UV) and ground images (visible) the solar rays of which are attenuated differently as they pass through the earth's atmosphere to illuminate the NLC/PMC.

8.4. New Low Latitude OMI Investigation

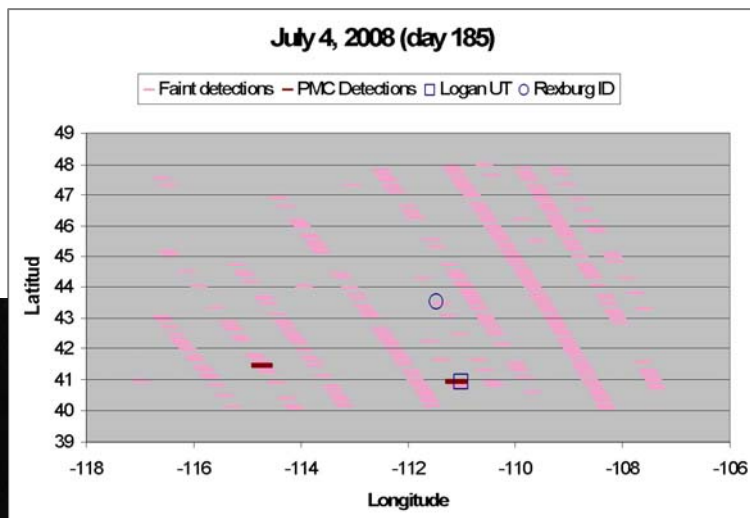
One very exciting aspect of OMI data is the fact that it regularly makes measurements down to latitudes of $\sim 35^\circ$. This allows for a investigation of coincident satellite ground-based measurements to a much greater extent than has previously been allowed. One night with coincident data has already been identified as described below.

8.4.1. Logan, UT, July 4/5, 2008 (day 186)

On the 4th of July 2008 an NLC display was reported from Rexburg, ID and Logan, UT. This was a faint display which was present at $\sim 4:00$ UT ($\sim 22:00$ LT) but the duration is not known. OMI data show good spatial coincidence that evening (red lines in Figure 31) with an albedo of $\sim 7 \times 10^{-6} \text{sr}^{-1}$. There were also several faint detections (indicated by pink lines) which show the spatial extent of the display. The OMI orbit (21109) passed over the area at $\sim 20:00$ UT (14:00 LT) so there is no temporal coincidence between the data sets on this occasion. However, the extensive OMI data suggest that this was a long lived display, although it was fainter than that observed from Logan in 1999 (Taylor et al., 2002).

The simple fact that OMI is able to distinguish PMC from foreground scattered light at low-latitudes ($< 50^\circ$) will open several avenues of research, especially projects directed at

Figure 31 OMI data from orbit 21109 on day 185 show spatial coincidence with visual and imaging reports from Logan UT (41°N , 111°W) and Rexburg ID (43.5°N , 111.5°W). The photograph below was taken from Rexburg, ID by B. R. Jordan



low latitude NLC displays.

9. References

- Benze, S., C.E. Randall, M.T. DeLand, G.E. Thomas, D.W. Rusch, S.M. Bailey, J.M. Russell, III, W. McClintock, A.W. Merkel, C. Jeppesen, Comparison of Polar Mesospheric Cloud Measurements from the Cloud Imaging and Particle Size Experiment and the Solar Backscatter Ultraviolet Instrument in 2007, *Journal of Atmospheric and Solar-Terrestrial Physics*, doi:10.1016/j.jastp.2008.07.014.
- Carbary J.F., Morrison D., Romick G. J., Ultraviolet Imaging and spectrographic imaging of polar mesospheric clouds, *Advanced Space Research Vol. 31, No. 9*, pp. 2091-2096, 2003
- Czechowsky, R. Ruster and G. Schmidt, Variations of mesospheric structures in different seasons, *Geophysical Research Letters* **6** (1979), pp. 459–462
- DeLand, M.T., E.P. Shettle, G.E. Thomas, and J.J. Olivero, Solar backscatter ultraviolet (SBUV) observations of polar mesospheric clouds (PMCs) over two cycles, *Journal of Geophysical Research*, 108(D8), 8445, 2003.
- DeLand M. T., E. P. Shettle, G. E. Thomas, J. J. Olivero, Latitude-dependent long-term variations in polar mesospheric clouds from SBUV version 3 PMC data, *Journal of Geophysical Research*, 112, D10315, 2007
- Donahue, T.M., Guenther, B., Blamont, J.E., Noctilucent clouds in daytime: circumpolar particulate layers near the summer mesopause, *Journal of Atmospheric Science* **29**, 1205, 1972
- Gadsden, M., Schröder, W., Noctilucent Clouds, Springer, Berlin, 1989.
- Gadsden, M., M. J. Taylor, Measurements of noctilucent cloud heights: a bench mark for changes in the mesosphere. *Journal of Atmospheric and Terrestrial Physics*, Vol. 56, No. 4, pp. 461-466, 1994
- Hemenway, C. L., Soberman, R. K., Witt, G. Sampling of noctilucent cloud particles, *Tellus*, 16, p. 84. 1964
- Jensen, E. J., Thomas, G.E., A growth sedimentation model of polar mesospheric clouds: Comparisons with SME measurements, *Journal of Geophysical Research*, Vol.93, 2461-2473, 1988.
- Jesse, O., Die Beobachtung der leuchtenden Wolken (Observations of noctilucent clouds), *Meteor. Z.*, 4, 179–181, 1887.
- Kirkwood, S., K. Stebel, The influence of planetary waves on Noctilucent cloud occurrence over NW Europe, *Journal of Geophysical Research* Submitted 22 March 2002
- Leslie, R. Sky Glows, *Nature*, 32, 245, 1885
- Merkel A.W., Rusch D., Palo S.E., Russell III J.M., Bailey S.M., Mesospheric planetary wave effects on global PMC variability inferred from AIM–CIPS and TIMED–SABER for the northern summer 2007 PMC season, *Journal of Atmospheric and Solar-Terrestrial Physics*, 71, 381–391, 2009

- Merkel, A.W. Thomas, G.E. Palo, S.E. Bailey, S.M. Observations of the 5-day planetary wave in PMC measurements from the Student Nitric Oxide Explorer Satellite, *Geophysical Research Letters*, Volume 30, Issue 4, pp. 45-1, 2003
- Rapp, M., Lübken, F.-J., Polar mesosphere summer echoes (PMSE): review of observations and current understanding. *Atmospheric Chemistry and Physics* 4, 2601-2633. 2004.
- Taylor, M.J., M. Gadsen, R.P. Lowe, M.S. Zalcik, J. Brausch, Mesospheric Cloud observations at unusually low latitudes, *Journal of Atmospheric and Solar-Terrestrial Physics* 64, 991-999, 2002.
- Taylor, M.J., Zhao Y. Pautet P.-D, Nicolls M.J., Collins R.L., Barker-Tvedtnes J.a., Burton C.D, Thurairajah B., Reimuller J., Varney R.H., Heinselman C.J., Mizutani K., etal., Coordinated optical and radar image measurements of Noctilucent clouds and polar mesospheric summer echoes, *Journal of Atmospheric and Solar-Terrestrial Physics*, 2009
- Thomas, G.E.,. Solar mesosphere explorer measurements of polar mesospheric clouds (Noctilucent clouds), *Journal of Atmospheric and Terrestrial Physics* 46, 819–824, 1984
- Thomas, G.E., Is the Polar Mesosphere the Miners Canary of Global Change?, *Advances in Space Research* 18, 149-158, 1996
- Thomas G.E., Are Noctilucent Clouds Harbingers of Global Change in the Middle Atmosphere, *Advanced Space Research Vol.32 No.9*, pp1737-1746, 2003
- Zalcik, M.S., A possible increase in mid-latitude sightings of noctilucent clouds, *Journal of the Royal Astronomical Society of Canada*, 92, 197-200, 1998

10. Author's Biography

Jodie Barker-Tvedtnes, grew up in Salt Lake City, Utah, and graduated in 2000 from Bingham High School. After taking two years away from school to raise her daughter, Kalila, Jodie entered the Salt Lake Community College to pursue a degree in English. Two years later in 2005, she transferred to the Department of Physics at Utah State University. During her time at USU, Jodie has also completed minors in Mathematics and in Classics with a Latin Emphasis. She has also taken advantage of the many opportunities for Undergraduate Research in the Physics Department, working with Dr. Michael Taylor for three years conducting research focused on the middle atmosphere. Through her efforts in Undergraduate Research and her participation in the local chapter of the Society of Physics Students (SPS), Jodie has been honored with several awards over the past four years. These include the Goldwater Scholarship (2008-2009) and the SPS Outstanding Undergraduate Researcher Award which gave her the opportunity to present her research in Krakow, Poland, at the 2008 International Conference for Physics Students.

After she graduates in May 2009, Jodie plans to begin a Doctorate Program in Space Physics at the University of California in Los Angeles.